Inorg. Chem. **2008**, *47*, 3034−3044

Ru and Os Complexes Containing a P,N-Donor Heterotopic Ligand: The Effect of Solvent on Stereochemistry

Serin L. Dabb,[†] Barbara A. Messerle,*[,†] Matthew K. Smith,[‡] and Anthony C. Willis[‡]

School of Chemistry, The University of New South Wales, Sydney, New South Wales, Australia, and Research School of Chemistry, The Australian National University, Canberra, ACT, Australia

Received September 25, 2007

Ruthenium and osmium complexes of the general formula $MCl_2(PyP)_2$ (where PyP is the P,N- donor ligand 1-(2-diphenylphosphinoethyl)pyrazole) were synthesized from $MCl_2(PPh_3)_3$ (where M = Ru or Os). Three of the five possible stereoisomers of $RuCl_2(PyP)_2$ were synthesized and characterized in solution by multinuclear NMR spectroscopy, and the structure of these in the solid state was determined by X-ray crystallography. Two of the analogous Os isomers were also synthesized. It was found that different solvents induced isomerization between these stereoisomers, indicating either lability of the chloride anion or hemilability of the PyP ligand. Bimetallic complexes of the general formula $[Ru(\mu\text{-}Cl)(PyP)_2]_2[X]_2$ were synthesized from chloride abstraction from $RuCl_2(PyP)_2$ using either silver ($X = OSO_2CF_3$, BF_4) or sodium ($X = BPh_4$) salts. The osmium analogue of the Ru bimetallic complexes, $[Os(\mu\text{-}Cl)(PyP)_2]_2[BPh_4]_2$, was also synthesized. Solid-state structures were obtained using X-ray crystallography for the osmium bimetallic complex and the ruthenium bimetallic complex where $X = OSO_2CF_3$. The hemilability of PyP was demonstrated through the synthesis of $RuCl_2(CO)(\kappa^1\text{-}P\text{-}PyP)(\kappa^2\text{-}P,N\text{-}PyP)$, which contains one pendant PyP ligand, bound through the P-donor atom.

Introduction

Bidentate P^N ligands, which contain both hard and soft donor atoms, have been used extensively in the synthesis of metal complexes. The differing electronic and structural properties of the donor atoms allow for tuning of the reactivity at the metal center, and as such, these ligand systems have great potential for use in catalysis. In particular, the potential hemilability of such ligands, where one donor group is substantially more labile than the other, is of interest in the development of catalysts as these ligand allow for the formation of reactive sites while maintaining the structure of the complex and protecting ability of the ligand.[1,2] Ruthenium complexes of the formula $RuCl_2(P^N)_2$ are effective catalysts for transfer hydrogenation[3–6] and also homocoupling of terminal alkynes.[7]

The majority of studies of metal complexes containing phosphine−nitrogen hybrid ligands have focused on phosphine−pyridine,[8,9] phosphine−oxazoline,[10,11] and, to a lesser extent, phosphine−imidazolyl[12] ligand systems (Figure 1). Only a limited number of phosphine−pyrazolyl bidentate donor ligands are known,[13–15] and the coordination chemistry of phosphine−pyrazolyl ligands, and their possible hemilability, has not been extensively studied. Pd,[16] Ru,[17,18] Fe[19] and Rh[20] metal complexes containing mixed phosphine−pyrazolyl ligands have been synthesized.

On binding of bidentate P^N donor ligands with a range of sp^2 N-donors to Ru and Os, octahedral complexes of the

* To whom correspondence should be addressed. E-mail: b.messerle@unsw.edu.au.
† The University of New South Wales.
‡ The Australian National University.

(1) Braunstein, P. *J. Organomet. Chem.* **2004**, *689*, 3953–3967.
(2) Guiry, P. J.; Saunders, C. P. *Adv. Synth. Catal.* **2004**, *346*, 497–537.
(3) Braunstein, P.; Graiff, C.; Naud, F.; Pfaltz, A.; Tiripichio, A. *Inorg. Chem.* **2000**, *39*, 4468–4475.
(4) Yang, H.; Lugan, N.; Mathieu, R. C. R. *C. R. Acad. Sci., Sér. IIc: Chim.* **1999**, *251*, 258.
(5) Dahlenburg, L.; Kuehnlein, C. *J. Organomet. Chem.* **2005**, *690*, 1–13.
(6) Rahman, M. S.; Prince, P. D.; Steed, J. W.; Hii, K. K. *Organometallics* **2002**, *21*, 4927–4933.
(7) Slugovc, C.; Doberer, D.; Gemel, C.; Schmid, R.; Kirchner, K.; Winkler, B.; Stelzer, F. *Monatsh. Chem.* **1998**, *129*, 221–233.
(8) Espinet, P.; Soulantica, K. *Coord. Chem. Rev.* **1999**, *193–195*, 499–556.
(9) Newkome, G. R. *Chem. Rev.* **1993**, *93*, 2067–2089.
(10) Helmchen, G.; Pfaltz, A. *Acc. Chem. Res.* **2000**, *33*, 336–345.
(11) Braunstein, P.; Naud, F. *Angew. Chem., Int. Ed.* **2001**, *40*, 680–699.
(12) Jalil, M. A.; Fujinami, S.; Senda, H.; Nishikawa, H. *J. Chem. Soc., Dalton Trans.* **1999**, 1655–1661.
(13) Caiazzo, A.; Dalili, S.; Yudin, A. K. *Org. Lett.* **2002**, *4*, 2597–2600.

10.1021/ic7019044 CCC: $40.75
Published on Web 03/18/2008

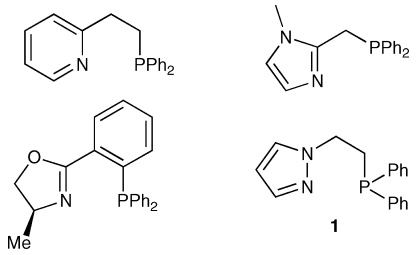

Figure 1

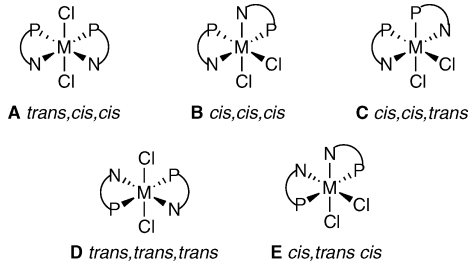

Figure 2

general formula $MCl_2(P^{\frown}N)_2$ have been reported. Five possible stereoisomers of $MCl_2(P^{\frown}N)_2$ have been established (Figure 2), with isomer **A** being the most common.[5,6,17,21–24] There are far fewer known examples of isomers **B**[25,26] and **E**[27] (Figure 2). Changes in metal precursor or ligand substituents can lead to the preferential formation of particular isomers. For example, addition of $P^{\frown}N$ ligands, where N is a pyridine moiety, to $RuCl_2(PPh_3)_3$ produced a mixture of isomers **A** and **B** (in two diastereomers) where the ratio of **A**:**B** was dependent on the nature of the substituents on the phosphorus or pyridine.[4] The addition of a (phosphinomethyl)oxazoline ligand to $RuCl_2(PPh_3)_3$ yielded isomer **B** exclusively; however, when the Ru precursor was changed to $[RuCl_2(COD)]_n$, a small percentage of isomer **D** was also formed. Increasing the bulkiness of the substituents on the oxazoline ring also led to the formation of isomers **B** and **D**.[3]

Scheme 1

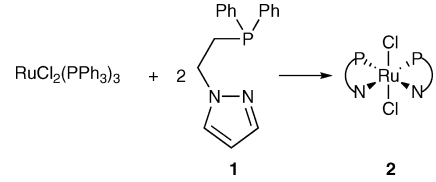

We have recently reported the synthesis of square planar Rh and Ir complexes containing the $P^{\frown}N$ ligand 1-(2-diphenylphospinoethyl)pyrazole (PyP, **1**, Scheme 1).[28] In order to provide insight into the coordination behavior of this potentially hemilabile bidentate ligand, we have also studied the reactivity of the PyP ligand with group 8 metals. In this paper we report the first example of the synthesis of three stereoisomers of the metal complex with general formula $RuCl_2(P^{\frown}N)_2$, where $P^{\frown}N$ = PyP (**1**), along with evidence of the hemilability of the PyP ligand. Crystal structures have been obtained for *trans*,*cis*,*cis*- (**2**), *cis*,*cis*,*cis*- (**3**), and *cis*,*cis*,*trans*-$RuCl_2(PyP)_2$ (**4**) and for the analogous *trans*,*cis*,*cis*-$OsCl_2(PyP)_2$ (**5**). *cis*,*cis*,*trans*-$OsCl_2(PyP)_2$ (**6**) was also synthesized. This is the first example of the synthesis and X-ray structure of a phosphino-pyrazolyl complex of Os, and one of only a few[29] examples of complexes of the form $OsCl_2(P^{\frown}N)_2$. Bimetallic species of the Ru and Os complexes were also synthesized through chloride labilization and abstraction to yield a series of complexes of the type $[Ru(\mu\text{-}Cl)(PyP)_2]_2[X]_2$ (X = OSO_2CF_3 (**7**), BF_4 (**8**), BPh_4 (**9**)), and $[Os(\mu\text{-}Cl)(PyP)_2]_2[BPh_4]_2$ (**10**). The effects of solvent on the synthesis of the complexes, and their subsequent isomerization, are also reported. Direct comparisons between the isomerization of the Ru and Os stereoisomers have been made, as well as their stabilities in solution.

Results and Discussion

Mononuclear Metal Complexes. Synthesis of *trans*,*cis*,*cis*-$RuCl_2(PyP)_2$ (2). The addition of dichloromethane (DCM) to a mixture of 1 equiv of $RuCl_2(PPh_3)_3$ and 2 equiv of **1**, with isolation using *n*-hexanes to remove the free PPh_3, gave *trans*,*cis*,*cis*-$RuCl_2(PyP)_2$ (**2**) cleanly and in good yields (Scheme 1). The order of addition of ligand and metal precursor in this reaction was important, as addition of a solution of ligand in dichloromethane to a solution of metal precursor in dichloromethane produced a small percentage of the *cis*,*cis*,*cis*-isomer **3** in addition to isomer **2**. The $^{31}P\{^1H\}$ NMR spectrum of isomer **2** exhibited the expected singlet at 34.4 ppm, due to the C_2 symmetry of the complex. In the ^1H NMR spectrum the resonances due to the two methylene protons on the ligand backbone ($-NCH_2CH_2P-$) appeared as broad singlets. The resonances due to the phenyl and pyrazolyl protons of the product have similar, but distinguishable, chemical shifts to those of the protons of the free ligand (Figure 6).

2 was also synthesized in a much lower yield on refluxing 1 mol equiv of $RuCl_2(PPh_3)_3$ with 2 mol equiv of PyP (**1**) in toluene.

(14) Abbenhuis, H. C. L.; Burckhardt, U.; Gramlich, V.; Togni, A.; Albinati, A.; Mueller, B. *Organometallics* **1994**, *13*, 4481–4493.
(15) Mukherjee, A.; Sarkar, A. *Tetrahedron Lett.* **2004**, *45*, 9525–9528.
(16) Grotjahn, D. B.; Combs, D.; Van, S.; Aguirre, G.; Ortega, F. *Inorg. Chem.* **2000**, *39*, 2080–2086.
(17) Esquius, G.; Pons, J.; Yanez, R.; Ros, J.; Mathieu, R.; Lugan, N.; Donnadieu, B. *J. Organomet. Chem.* **2003**, *667*, 126–134.
(18) Espino, G.; Jalon, F. A.; Maestro, M.; Manzano, B. R.; Perez-Manrique, M.; Bacigalupe, A. C. *Eur. J. Inorg. Chem.* **2004**, 2542–2552.
(19) Tribo, R.-M.; Ros, J.; Pons, J.; Yanez, R.; Alvarez-Larena, A.; Piniella, J.-F. *J. Organomet. Chem.* **2003**, *676*, 38–42.
(20) Esquius, G.; Pons, J.; Yanez, R.; Ros, J.; Mathieu, R.; Donnadieu, B.; Lugan, N. *Eur. J. Inorg. Chem.* **2002**, 2999–3006.
(21) Crochet, P.; Gimeno, J.; Borge, J.; Garcia-Granda, S. *New J. Chem.* **2003**, *27*, 414–420.
(22) Abdur-Rashid, K.; Guo, R.; Lough, A. J.; Morris, R. H.; Song, D. *Adv. Synth. Catal.* **2005**, *347*, 571–579.
(23) Guo, Z.; Habtemariam, A.; Sadler, P. J.; James, B. R. *Inorg. Chim. Acta* **1998**, *273*, 1–7.
(24) Morris, R.; Habtemariam, A.; Guo, Z.; Parsons, S.; Sadler, P. J. *Inorg. Chim. Acta* **2002**, *339*, 551–559.
(25) Caballero, A.; Jalon, F. A.; Manzano, B. R.; Sauthier, M.; Toupet, L.; Reau, R. *J. Organomet. Chem.* **2002**, *663*, 118–126.
(26) Drommi, D.; Nicolo, F.; Arena, C. G.; Bruno, G.; Faraone, F.; Gobetto, R. *Inorg. Chim. Acta* **1994**, *221*, 109–116.
(27) Quirmbach, M.; Holz, J.; Tararov, V. I.; Borner, A. *Tetrahedron* **2000**, *56*, 775–780.
(28) Burling, S.; Field, L. D.; Messerle, B. A.; Vuong, K. Q.; Turner, P. *Dalton Trans.* **2003**, 4181–4191.
(29) Del Zotto, A.; Mezzetti, A.; Rigo, P. *J. Chem. Soc., Dalton Trans.* **1994**, 2257–2264.
(30) Costella, L.; Del Zotto, A.; Mezzetti, A.; Zangrando, E.; Rigo, P. *J. Chem. Soc., Dalton Trans.* **1993**, 3001–3008.

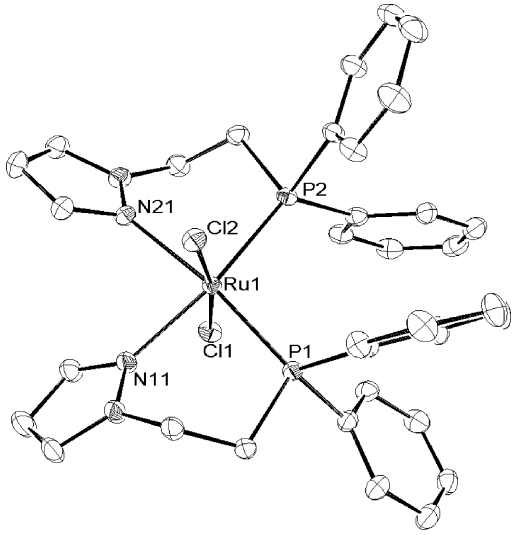

Figure 3. ORTEP depiction of **2** at 30% probability levels. H atoms have been omitted for clarity.

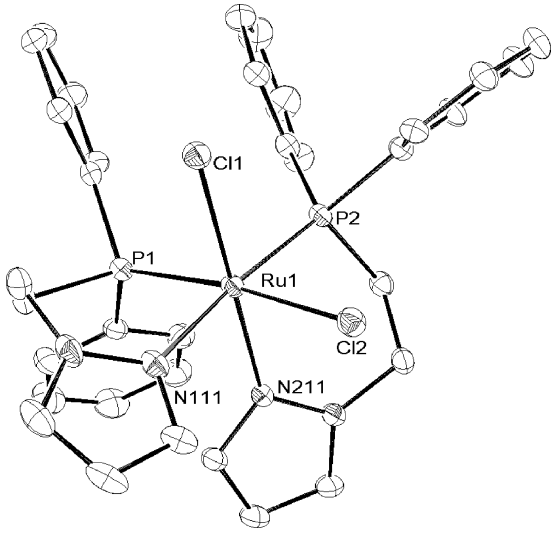

Figure 4. ORTEP depiction of **3** at 30% probability levels. H atoms have been omitted for clarity.

Table 1. Selected Bond Angles and Bond Lengths for the Solid-State Structures of **2**

Bond Lengths (Å)			
Ru(1)−Cl(1)	2.4170(9)	Ru(1)−Cl(2)	2.4245(9)
Ru(1)−P(1)	2.2861(2)	Ru(1)−P(2)	2.3103(9)
Ru(1)−N(11)	2.157(3)	Ru(1)−N(21)	2.161(3)
Bond Angles (deg)			
Cl(1)−Ru(1)−Cl(2)	171.38(3)	P(1)−Ru(1)−N(11)	88.31(8)
P(1)−Ru(1)−N(21)	170.55(8)	P(2)−Ru(1)−N(21)	87.41(8)
P(2)−Ru(1)−N(11)	169.54(8)		

On addition of PyP (**1**) to $RuCl_2(DMSO)_4$ in dichloromethane at room temperature, an inseparable mixture of products was formed. A view of the structure of **2**, as determined by X-ray crystallography, is shown in Figure 3, together with the atomic numbering system; selected bond distances and angles are given in Table 1.

Synthesis of *cis*,*cis*,*cis*-$RuCl_2(PyP)_2$ (3). 3 was synthesized by stirring a suspension of **2** in EtOH overnight. The product exhibited a pair of doublets in an AB splitting pattern in the $^{31}P\{^1H\}$ spectrum, with a $^2J_{PP}$ coupling of 37 Hz. The only isomer matching this splitting pattern is **3**, which was confirmed as the product by X-ray crystallography. A view of the structure of **3** is shown in Figure 4, together with the atomic numbering system; selected bond lengths and angles are given in Table 2. The formation of isomer **3** was also observed during the synthesis of isomer **2**. Isomer **3** is only sparingly soluble in tetrahydrofuran, acetone, and chloroform, unlike isomers **2** and **4**, which showed much higher solubilities in these solvents. As **3** readily isomerizes in solution, it could not be isolated as a pure sample. Microanalysis was performed on a clean mixture of **3** and **2** and NMR and mass spectroscopic data were acquired on a mixture of isomer **2** and **4**.

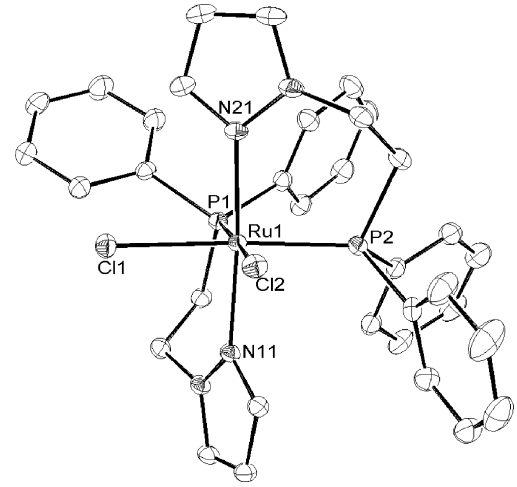

Figure 5. ORTEP depiction of **4** at 30% probability levels. H atoms have been omitted for clarity.

Table 2. Selected Bond Angles and Bond Lengths for the Solid-State Structure of **3**

Bond Lengths (Å)			
Ru(1)−Cl(1)	2.4314(11)	Ru(1)−Cl(2)	2.4989(12)
Ru(1)−P(1)	2.2742(12)	Ru(1)−P(2)	2.2871(11)
Ru(1)−N(111)	2.181(3)	Ru(1)−N(211)	2.079(3)
Bond Angles (deg)			
N(111)−Ru(1)−P(2)	173.40(10)	P(1)−Ru(1)−N(111)	89.23(10)
N(211)−Ru(1)−Cl(1)	175.66(9)	P(2)−Ru(1)−N(211)	92.06(9)
P(1)−Ru(1)−Cl(2)	170.98(4)	Cl(1)−Ru(1)−Cl(2)	90.41(4)

Due to the inequivalence of the two PyP ligands on the metal center of isomer **3** (one P is trans to N and one is trans to Cl), we would expect at least four separate resonances for the methylene protons ($-NCH_2CH_2P-$) on the ethyl backbone. The geminal protons on each carbon are also pairwise inequivalent and therefore the resonances due to the methylene protons of isomer **3** appear as eight distinct resonances all integrating to one proton (Figure 6c).

Synthesis of *cis*,*cis*,*trans*-$RuCl_2(PyP)_2$ (4). Heating the Ru isomer **2** to reflux in EtOH for 1.5 h yielded **4**. The product **4** was also obtained by stirring isomer **2** in EtOH for 48 h at room temperature. As expected the $^{31}P\{^1H\}$ NMR spectrum exhibited a singlet, with only a slight difference in chemical shift from the equivalent resonance observed for the *trans*,*cis*,*cis*-isomer **2**. The ^1H NMR spectrum of **4** is similar to that of the *trans*,*cis*,*cis*-isomer **2** as the two ligands are chemically and magnetically equivalent. However, the protons of the phenyl groups and $-NCH_2-$ protons within the ligand are magnetically inequivalent, as indicated by two-dimensional ^1H NMR spectroscopy and observed in the spectra of the *cis*,*cis*,*cis*-isomer **3**. The resonances due to the protons of the two phenyl rings of PPh_2 exhibit two sets of chemical shifts. The chemical shifts of the resonances due to the protons of the $-PCH_2$ groups appear at one chemical shift, but the resonances due to the $-NCH_2$ protons appear as two multiplets, each with an integration of one proton (Figure 6b).

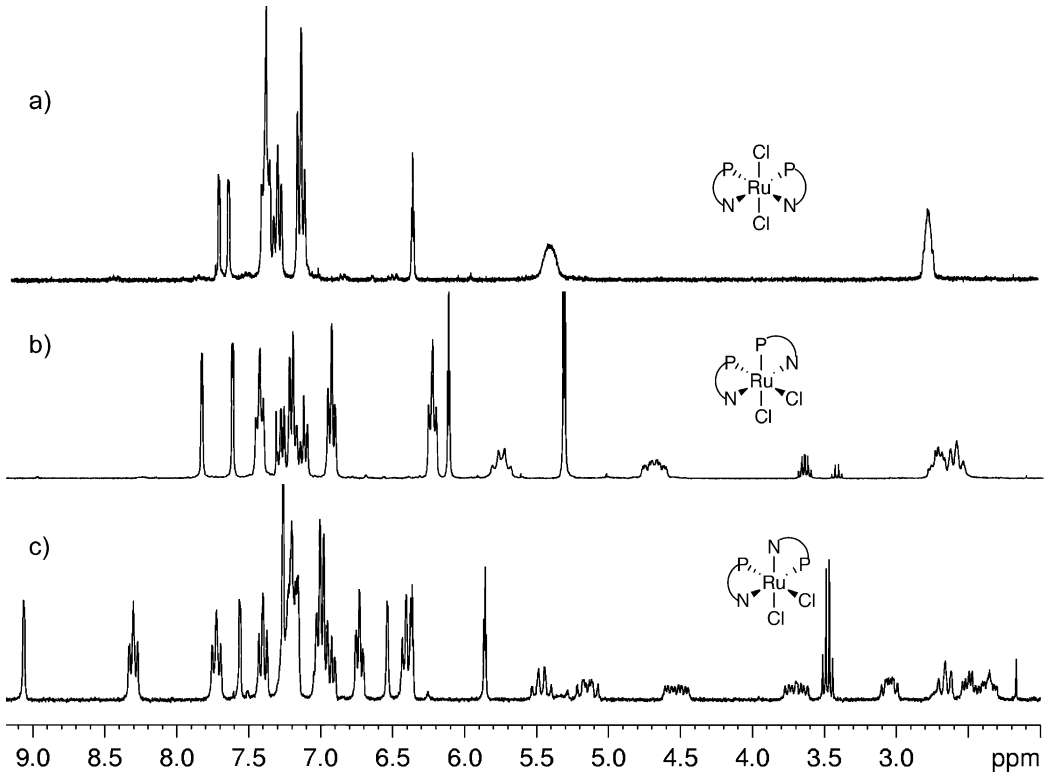

Figure 6. ^{1}H NMR spectra of (a) trans,cis,cis-isomer **2** in CD_2Cl_2, (b) *cis*,*cis*,*trans*-isomer **4** in CD_2Cl_2, and (c) *cis*,*cis*,*cis*-isomer **3** in $CDCl_3$ at 298 K, 300 MHz.

Table 3. Selected Bond Angles and Bond Lengths for the Solid-State Structure of **4**

molecule a		molecule b	
Bond Lengths (Å)			
Ru(1)−Cl(1)	2.4883(5)	Ru(2)−Cl(3)	2.4815(5)
Ru(1)−P(1)	2.2915(5)	Ru(2)−P(3)	2.2934(5)
Ru(1)−N(11)	2.1016(15)	Ru(2)−N(31)	2.1035(16)
Ru(1)−Cl(2)	2.4907(5)	Ru(2)−Cl(4)	2.4752(5)
Ru(1)−P(2)	2.2808(5)	Ru(2)−P(4)	2.2794(6)
Ru(1)−N(21)	2.1042(15)	Ru(2)−N(41)	2.1053(17)
Bond Angles (deg)			
Cl(2)−Ru(1)−P(1)	177.22(18)	Cl(3)−Ru(2)−P(4)	174.21(19)
Cl(1)−Ru(1)−P(2)	170.54(19)	Cl(4)−Ru(2)−P(3)	174.98(2)
N(11)−Ru(1)−N(21)	174.36(6)	N(31)−Ru(2)−N(41)	173.33(6)
P(1)−Ru(1)−N(11)	93.31(5)	P(3)−Ru(2)−N(31)	93.40(5)
P(2)−Ru(1)−N(21)	92.93(5)	P(4)−Ru(2)−N(41)	93.20(5)
Cl(1)−Ru(1)−Cl(2)	82.84(17)	Cl(3)−Ru(2)−Cl(4)	86.76(19)
P(1)−Ru(1)−P(2)	94.74(19)	P(3)−Ru(2)−P(4)	96.43(19)

The solid-state structure of **4** was also determined using X-ray crystallography. The crystals consisted of two crystallographically independent but almost identical molecules (a and b). A view of the structure of one of the molecules (a) is shown in Figure 5, together with the atomic numbering system; selected bond lengths and angles are give in Table 3.

Synthesis of *trans*,*cis*,*cis*-$OsCl_2(PyP)_2$ (5) and *cis*,*cis*,*trans*-$OsCl_2(PyP)_2$ (6). The *trans*,*cis*,*cis*-isomer of **5** was synthesized in the same manner as the analogous Ru compound **2** by addition of dichloromethane to a mixture of 1 mol equiv of $OsCl_2(PPh_3)_3$ and 2 mol equiv of PyP with stirring at room temperature for 5 h. The order of addition of ligand and metal precursor in this case was not important, with clean product being formed in high yields whether solvent was added to a mixture of the starting materials or a solution of the ligand was added slowly to $OsCl_2(PPh_3)_3$.

The ^{1}H NMR spectrum exhibited the expected peaks attributed to the protons of the **1** ligand, with the resonances due to the protons on the ethyl backbone appearing at 5.29 and 2.67 ppm for the $-NCH_2$ and $-PCH_2$ groups, respectively, and was similar to the spectrum of the analogous Ru compound **2**. The ^{31}P NMR spectrum showed the expected singlet but with a significantly different chemical shift at −28.2 ppm to those of the equivalent ruthenium compounds.

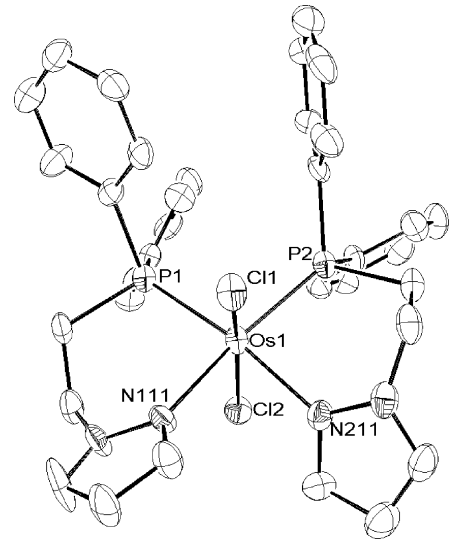

Figure 7. ORTEP depiction of *trans*,*cis*,*cis*-$OsCl_2(PyP)_2$ (**5**) at 30% probability levels. H atoms have been omitted for clarity.

The solid-state structure of **5** was characterized by X-ray crystallography. The crystals consisted of two crystallographically independent but almost identical molecules (a and b). A view of the structure of molecule a of **5** is shown in Figure 7, together with the atomic numbering system; selected bond lengths and angles are given in Table 4.

Table 4. Selected Bond Angles and Bond Lengths for the Solid-State Structure of **5**

molecule a		molecule b	
Bond Lengths (Å)			
Os(1)−Cl(1)	2.431(3)	Os(2)−Cl(3)	2.436(3)
Os(1)−P(1)	2.276(3)	Os(2)−P(3)	2.289(3)
Os(1)−N(111)	2.150(8)	Os(2)−N(311)	2.149(9)
Os(1)−Cl(2)	2.435(3)	Os(2)−Cl(4)	2.432(3)
Os(1)−P(2)	2.289(3)	Os(2)−P(4)	2.294(3)
Os(1)−N(211)	2.179(9)	Os(2)−N(411)	2.155(9)
Bond Angles (deg)			
N(211)−Os(1)−P(1)	171.9(3)	N(411)−Os(2)−P(3)	171.8(3)
N(111)−Os(1)−P(2)	171.1(2)	N(311)−Os(2)−P(4)	170.6(3)
Cl(1)−Os(1)−Cl(2)	165.79(10)	Cl(3)−Os(2)−Cl(4)	168.43(10)
P(1)−Os(1)−N(111)	89.5(2)	N(311)−Os(2)−P(3)	88.9(3)
P(2)−Os(1)−N(211)	88.4(3)	P(4)−Os(2)−N(41)	87.4(3)

Scheme 2

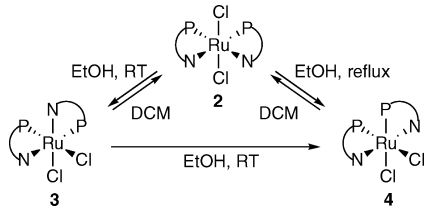

6 was synthesized in a similar manner to the analogous Ru isomer **4**, with refluxing in EtOH for 2 h. Complex **6** was characterized fully by NMR spectroscopy, mass spectroscopy, and microanalysis. The ^{1}H NMR spectrum of **6** mimics that of ruthenium complex **4**, with the protons of the phenyl groups and the geminal $-NCH_2-$ protons within the ligand being magnetically inequivalent. The ^{31}P NMR spectrum exhibits a singlet at −22.4 ppm, which shows the same upfield trend as the osmium isomer **5**.

Exchange between Isomers of $RuCl_2(PyP)_2$ and $OsCl_2(PyP)_2$. It was found that isomerization of $RuCl_2(PyP)_2$ can be induced through changes in the reaction conditions, such as solvent and temperature (Scheme 2), as observed by NMR spectroscopy.

In solution both **3** and **4** are less stable toward isomerization than isomer **2**, with both species isomerizing completely into **2** in chlorinated solvents (such as dichloromethane and chloroform). In ethanol complex **2** isomerizes to complex **3** at room temperature overnight; complex **3** then further isomerizes to complex **4** after another 24 h at room temperature in ethanol. In both chloroform and dichloromethane, complex **3** converts back to a mixture of isomers **2** and **3**, with full conversion of **3** to **2** after 2 days. The *trans*,*cis*,*cis*-isomer **2** converts fully to the *cis*,*cis*,*trans*-isomer **4** upon refluxing in ethanol for a few hours. Isomer **4** is stable in chlorinated solvents for 2 days but converts almost entirely back to the *trans*,*cis*,*cis*-isomer **2** after a week at room temperature in dichloromethane. The three isomers **2**, **3**, and **4** exhibit no isomerization in tetrahydrofuran or acetone.

5 converts to **6** upon refluxing in ethanol, in a similar fashion to the ruthenium analogue **2**. *cis*,*cis*,*cis*-$OsCl_2(PyP)_2$ was observed by NMR spectroscopy upon allowing **6** to stand in a $CDCl_3$ solution over 1 week, but attempts to isolate this complex led only to recovery of the original isomer **6**. The *cis*,*cis*,*trans*-isomer **6** was synthesized cleanly, and was stable toward isomerization in CD_2Cl_2 solutions, unlike the analogous ruthenium complex **4**.

The isomerization of the Ru complexes in solution was also investigated in the presence of excess tetrabutylammonium chloride, which is a source of chloride ions. The presence of [*n*-Bu_4N]Cl is expected to suppress isomerization of the ruthenium complexes if the isomerization process is due to labilization of the Cl^- coligand. Solutions of isomer **4** in dichloromethane and isomer **2** in ethanol

Scheme 3

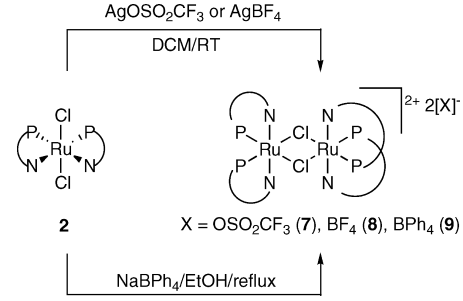

were monitored for conversion to isomer **2** and **4**, respectively, with and without the addition of excess [*n*-Bu_4N]Cl. The formation of isomer **2** from isomer **4** in dichloromethane was significantly slower in the presence of [*n*-BuN_4]Cl, as isomer **4** was still present in the solution after 7 days whereas isomer **4** was fully converted to isomer **2** after only 5 days when no tetrabutylammonium chloride was added. Similar suppression of isomerization was seen for the complex **2**, where a mixture of isomers **3** and **4** was formed in a ratio of 2:5, respectively, after leaving a mixture of [*n*-Bu_4N]Cl and isomer **2** in EtOH after 22 h, and isomer **2** was converted fully to isomer **4** in the absence of [*n*-BuN_4]Cl after the same time.

Binuclear Complexes of Ru and Os. A series of complexes with the general formula $[Ru(\mu\text{-}Cl)](PyP)_2]_2[X]_2$ (where X = OSO_2CF_3, BF_4, or BPh_4) was synthesized by three different methods (Scheme 3).

Upon addition of 1 equiv of either $AgOSO_2CF_3$ or $AgBF_4$ to a solution of **2** in dichloromethane and after removal of AgCl by filtration, the complexes $[Ru(\mu\text{-}Cl)(PyP)_2]_2[X]_2$ (where X = OSO_2CF_3 (**7**) or BF_4 (**8**)) were isolated in good yields (Scheme 3). The product **7** was fully characterized, with X-ray crystallography confirming the dimeric structure of the complex. Addition of $AgOSO_2CF_3$ to the *cis*,*cis*,*trans*-isomer (**4**) yielded the same product (**7**) as the addition of $AgOSO_2CF_3$ to the *trans*,*cis*,*cis*-isomer (**2**). $TlOSO_2CF_3$ was also used instead of $AgOSO_2CF_3$ to yield **7** under the same reaction conditions.

It was established that silver salts were not necessary for chloride abstraction. When *trans,cis,cis*-$RuCl_2(PyP)_2$ (**2**) was refluxed in EtOH with 1 equiv of $NaBPh_4$, the dimeric complex $[Ru(\mu\text{-}Cl)(PyP)_2]_2[BPh_4]_2$ (**9**) was formed in good yield. Performing the reaction in dichloromethane at room temperature yielded only starting material. The BPh_4^- analogue was also synthesized through counterion displacement, where $NaBPh_4$ was added to $[Ru(\mu\text{-}Cl)(PyP)_2]_2[OSO_2CF_3]_2$ (**7**) in dichloromethane to produce $[Ru(\mu\text{-}Cl)(PyP)_2]_2[BPh_4]_2$ (**9**).

The NMR spectra of all of the binuclear complexes were similar (not including differences due to the resonances due to the counterions). The bimetallic species has a similar geometry to the monomeric *cis*,*cis*,*trans*-isomer **4**, with both P nuclei trans to a Cl^-, and the N-donor atoms of the ligand both trans to each other. $^{31}P\{^1H\}$ spectra contained one singlet at a similar chemical shift to that of the Ru starting material **2**. The inequivalence of the resonances due to the protons of the two Ph rings of $-PPh_2$ in the ^{1}H NMR spectrum indicated that the rings are unable to rotate freely, most likely due to significant steric hindrance. The rigidity of the ethyl backbone of the ligand seen in the *cis*,*cis*,*cis*- and *cis*,*cis*,*trans*-isomers is not apparent in the dimer, with the resonances due to the pairs of geminal protons of each methylene group of the complexes **7**, **8**, and **9** being magnetically equivalent.

The *m*/*z* peak due to the cationic species $[RuCl(PyP)_2]^+$ (or $[Ru(\mu\text{-}Cl)(PyP)_2]_2^{2+}$) was observed by mass spectrometry for complexes **7** and **9**.

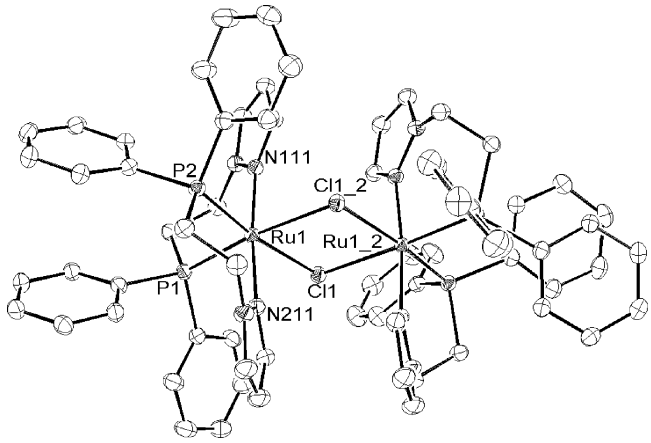

Figure 8. ORTEP depiction of $[Ru(\mu\text{-}Cl)(PyP)_2]_2^{2+}$, the cation of **7**. H atoms have been omitted for clarity. Atom Ru1_2 was generated by symmetry.

Table 5. Selected Bond Angles and Bond Lengths for the Solid-State Structure of $[Ru(\mu\text{-}Cl)(PyP)_2]_2$ $[OSO_2CF_3]_2$ (**7**)[a]

	Bond Lengths (Å)		
Ru(1)−Cl(1)	2.4774(14)	Ru(1)−P(2)	2.2915(8)
Ru(1)−P(1)	2.2859(14)	Ru(1)−N(211)	2.111(2)
Ru(1)−N(111)	2.110(2)		
	Bond Angles (deg)		
Cl(1)−Ru(1)−P(1)	92.40(13)	Ru(1)#1-Cl(1)−Ru(1)	99.68(3)
Cl(1)−Ru(1)−P(2)	171.73(2)	P(1)−Ru(1)−P(2)	95.59(3)
N(111)−Ru(1)−N(211)	174.72(8)	P(2)−Ru(1)−N(211)	93.71(6)
P(1)−Ru(1)−N(111)	93.54(6)	Cl(1)−Ru(1)−Cl(1)#1	80.32(3)

[a] Atoms labeled with #1 were generated by symmetry.

The solid-state structure of $[Ru(\mu\text{-}Cl)(PyP)_2]_2[OSO_2CF_3]_2$ (**7**) was determined using X-ray crystallography. A view of the structure of the cation is shown in Figure 8, together with the atomic numbering system; selected bond distances and angles are given in Table 5.

The synthesis of the Os bimetallic species, $[Os(\mu\text{-}Cl)(PyP)_2]_2[X]_2$, could only be achieved via addition of a sodium salt to **5**. Reaction of *trans*,*cis*,*cis*-$OsCl_2(PyP)_2$ (**5**) with $AgOSO_2CF_3$ gave a paramagnetic Os(III) species as indicated by a very broad ^1H NMR spectrum, and mass spectroscopy confirmed that the product contained the $[OsCl_2(PyP)_2]^+$ ion. It was concluded that Ag^+ had oxidized the Os(II) starting material; however, reaction with $TlOSO_2CF_3$, which is not regarded as an oxidizing reagent, yielded the same result. $[Os(\mu\text{-}Cl)(PyP)_2]_2[BPh_4]_2$ (**10**) was synthesized by refluxing **5** and $NaBPh_4$ in EtOH to give a product with comparable spectroscopic and structural properties to the Ru analogue **9**. The difference in chemical shift of the phosphorus resonance in the ^{31}P NMR spectra of the Ru and Os monomeric species **2** and **5** was mirrored in the bimetallic species, as the Os dimer **10** exhibited a singlet at a far higher field (−20.5 ppm) than that of the Ru analogue **9** (35.1 ppm).

The solid-state structure of $[Os(\mu\text{-}Cl)(PyP)_2]_2[BPh_4]_2$ (**10**) was determined using X-ray crystallography. A view of the structure is shown in Figure 9, together with the atomic numbering system; selected bond distances and angles are given in Table 6.

The complex $RuCl(OSO_2CF_3)(PyP)_2$ could not be synthesized through chloride substitution in **2**, nor did we see dissociation of the bimetallic species of either Ru or Os into the five-coordinate complex $[MCl(PyP)_2][X]$. Low-temperature (<210 K) NMR studies yielded no evidence of an equilibrium existing between the dimeric and monomeric complexes in solution.

Structural Information. Solid-state structures determined by X-ray crystallography were obtained for the three isomers of

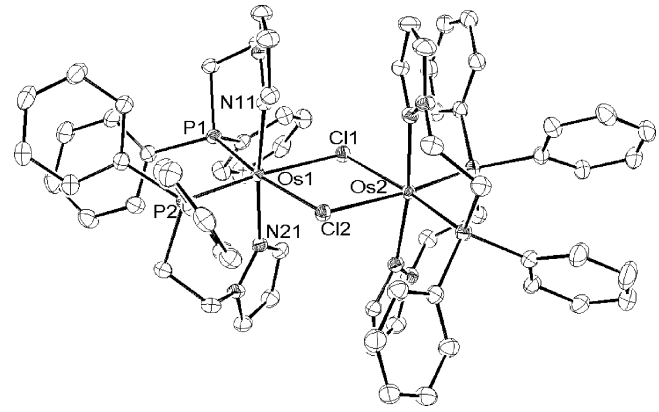

Figure 9. ORTEP depiction of the cation of $[Os(\mu\text{-}Cl)(PyP)_2]_2[BPh_4]_2$ (**10**) at 30% probability levels. H atoms have been omitted for clarity.

Table 6. Selected Bond Angles and Bond Lengths for the Solid-State Structure of $[Os(\mu\text{-}Cl)(PyP)_2]_2[BPh_4]_2$ (**10**)[a]

	Bond Lengths (Å)		
Os(1)−Cl(1)	2.4875(8)	Os(1)−Cl(2)	2.5066(7)
Os(1)−P(1)	2.2805(8)	Os(1)−P(2)	2.2757(8)
Os(1)−N(11)	2.114(3)	Os(1)−N(21)	2.118(3)
	Bond Angles (deg)		
Cl(1)−Os(1)−P(1)	92.37(3)	Os(1)−Cl(1)−Os(2)	101.46(3)
Cl(1)−Os(1)−P(2)	171.41(3)	P(1)−Os(1)−P(2)	96.22(3)
N(11)−Os(1)−N(21)	174.09(10)	P(2)−Os(1)−N(21)	92.86(8)
P(1)−Os(1)−N(11)	93.27(8)	Cl(1)−Os(1)−Cl(2)	78.51(2)

[a] Only one-half of the atoms of the dimer are represented due to symmetry of the molecule.

$RuCl_2(PyP)_2$ (**2**, **3**, and **4**), and also for *trans*,*cis*,*cis*-$OsCl_2(PyP)_2$ (**5**), $[Ru(\mu\text{-}Cl)(PyP)_2]_2[OSO_2CF_3]_2$ (**7**), and $[Os(\mu\text{-}Cl)(PyP)_2]_2$-$[BPh_4]_2$ (**10**). Suitable crystals were grown by slow diffusion of a nonpolar solvent (either *n*-pentane or *n*-hexanes) into a concentrated dichloromethane or acetone solution of the compound. Crystallographic data for all six compounds are given in Table 7.

The crystallographic asymmetric unit of each complex contained at least one molecule of solvent: dichloromethane and/or water, *n*-pentane, or acetone. These are specified in the crystallographic table (Table 7). The crystallographic asymmetric unit of isomer **3** consists of one molecule of $RuCl_2(PyP)_2$ and one highly disordered molecule of *n*-pentane. (The displacement parameters of the *n*-pentane molecule have been left isotropic since the disorder could not be modeled well). The *trans*,*cis*,*cis*-isomers for Ru (**2**) and Os (**5**) have a pseudo C_2 symmetry axis that bisects the N−M−N angle and P−M−P angles. Although Ru isomer **4** has no crystallographically imposed symmetry in the solid-state, it shows an approximate C_2 symmetry with the pseudo-2-fold axis bisecting the Cl−Ru−Cl and P−Ru−P angles.

The Ru−Cl, Ru−P, and Ru−N bond lengths in the isomers **2**, **3**, and **4** of $RuCl_2(PyP)_2$ are typical for complexes of the type $RuCl_2(P^{\frown}N)_2$ with values between 2.42 and 2.50, 2.26 and 2.31, and 2.08 and 2.18 Å, respectively. Complexes of this general formula also typically have a distorted octahedral geometry, as indicated by axial bond angles less than the ideal 180°.[3,4,17,21,24,26] Axial bond angles as low as 158.4(1)° have been observed for *cis*,*cis*,*cis*-$RuCl_2(P^{\frown}N)_2$ (isomer **C**), where P⌒N was the ligand 2-(diphenylphosphino)pyridine with a short P⌒N bridge.[26] All three isomers presented here, however, exhibit average axial bond angles with values between 169.54 and 177.22°. This general lack of high distortion from the ideal angle of 180° seen across all three isomers indicates there is no reason (due to steric strain) why one isomer should be formed preferentially over another.

Table 7. Crystallographic Data for *trans*,*cis*,*cis*-$RuCl_2(PyP)_2$ (**2**), *cis*,*cis*,*cis*-$RuCl_2(PyP)_2$ (**3**), *cis*,*cis*,*trans*-$RuCl_2(PyP)_2$ (**4**), *trans*,*cis*,*cis*-$OsCl_2(PyP)_2$ (**5**), $[Ru(\mu\text{-}Cl)(PyP)_2]_2[OSO_2CF_3]_2$ (**7**), and $[Os(\mu\text{-}Cl)(PyP)_2]_2[BPh_4]_2$ (**10**)

	2	**3**	**4**	**6**	**5**	**9**
empirical formula	**2**·1.5(CH_2Cl_2)·0.25(H_2O)	**3**·(*n*-pentane)	**4**·1.5(CH_2Cl_2)	**6**·6(CH_2Cl_2)	**5**·2(CH_2Cl_2)	**9**·4(C_3H_6O)
M (g mol^{-1})	864.50	792.61	1719.98	2201.92	1813.24	2443.33
crystal system	orthorhombic	monoclinic	monoclinic	monoclinic	monoclinic	monoclinic
space group	*Pccn*	$P2_1/n$	$P2_1/n$	$C2/c$	$P2_1/n$	$P2_1/n$
a (Å)	18.5441(3)	11.656(2)	15.0764(1)	33.779(7)	10.250(2)	18.4958(1)
b (Å)	39.6000(6)	15.015(3)	17.1534(1)	12.670(3)	19.019(4)	30.2710(2)
c (Å)	10.2814(2)	21.886(4)	28.8099(3)	26.597(5)	37.938(8)	20.4361(2)
b (deg)		98.44(3)	100.6436(3)	126.83(4)	92.48(3)	97.2536(4)
V (Å ^{3})	7550.1(2)	3789.1(13)	7322.39(8)	9111(3)	7389(3)	11350.32(15)
D_c (g·cm^{-3})	1.521	1.389	1.560	1.605	1.630	1.430
Z	8	4	8	4	4	4
T (K)	200(2)	200(2)	200(2)	200(2)	200(2)	200(2)
λ (Mo Kα) (Å)	0.71073	0.71073	0.71073	0.71073	0.71073	0.71073
μ (Mo Kα) (mm^{-1})	0.887	0.672	0.913	0.925	3.858	2.398
crystal size (mm)	0.37 × 0.25 × 0.09	0.14 × 0.13 × 0.12	0.50 × 0.28 × 0.19	0.21 × 0.15 × 0.14	0.14 × 0.12 × 0.09	0.47 × 0.38 × 0.21
crystal color	yellow	yellow	yellow	yellow	yellow	orange
crystal habit	plate	cube	plate	prism	prism	plate
$2\theta_{max}$ (deg)	55	55	55	55	55	55
hkl range	−23 → 24	−15 → 15	−19 → 19	−43 → 43	−12 → 12	−23 → 24
	−51 → 46	−19 → 18	−22 → 22	−16 → 16	−22 → 20	−39 → 39
	−13 → 13	−28 → 28	−37 → 37	−34 → 31	−45 → 44	−26 → 26
N	87165	72220	145653	97540	62906	191655
N_{ind}	8647	8672	16722	10432	12347	25984
	(R_{merge} 0.075)	(R_{merge} 0.098)	(R_{merge} 0.039)	(R_{merge} 0.056)	(R_{merge} 0.069)	(R_{merge} 0.059)
N_{obs} ($I > 2\theta(I)$)	4654	6120	13871	7969	9152	18018
GoF(all)	0.992	1.036	0.957	0.991	1.230	0.956
R1[a] (F, $I > 2\sigma(I)$)	0.0270	0.0489	0.0279	0.0414	0.0679	0.0242
wR2[b] (F^2, all data)	0.0993	0.0828	0.0759	0.0600	0.1025	0.0733

[a] $R1 = \sum||F_o| - |F_c||/\sum|F_o|$ for $F_o > 2\sigma(F_o)$. [b] $wR2 = (\sum w(F_o^2 - F_c^2)^2/\sum(wF_c^2)^2)^{1/2}$ all reflections.

The synthesis of a series of stereoisomers of $RuCl_2(PyP)_2$ enables us to compare bond lengths for Ru−Cl, −P, and −N trans to each of the donor atoms N, P, and Cl. It is expected that all bonds trans to P will be long, due to the high trans influence of P relative to Cl and N donor ligands. Cl- and N-donor ligands have similar trans influences, with halides being slightly stronger.[34,35] The Ru−N bond lengths, which demonstrate the most distinctive trend across **2**, **3**, and **4**, do not show this predicted pattern, with bonds trans to Cl being shorter than those trans to N. Similarly, the Ru−Cl bond lengths are shortest when trans to Cl, and comparable when trans to either P or N. Ru−P bonds trans to either N or Cl give comparable lengths. P-donors do not occur trans to each other in any of the isomers due to phosphorus's high trans influence.

The higher than expected trans influence of the pyrazole moiety could induce ligand dissociation which would contribute to the ability of ruthenium complexes containing PyP (**1**) to isomerize in solution.

trans,*cis*,*cis*-Osmium complex **5** has very similar crystallographic properties to its Ru analogue **2**. The M−Cl, M−N, and M−P bond lengths and P−M−N bite angles of the PyP ligand are almost identical in **2** and **5**. The only significant differences are the Cl−M−Cl bond angles, with the osmium complex **5** showing greater distortion from the ideal octahedral geometry (165.79(10) and 168.43(10) Å compared to 171.38(3) Å for **2**). This can be attributed to the larger atomic radius of its metal center.

As mentioned earlier, the dimeric species **7** and **10** have the same configuration about the metal center as the *cis*,*cis*,*trans*-isomers **4** and **6**, with both P atoms trans to Cl. The complexes have three 2-fold axes of symmetry, one through Cl···Cl and M···M and one perpendicular to the MCl_2M plane, which is seen in similar compounds reported previously.[30] The structure of the Os dimer **10** was analogous to the structure of the Ru dimer **7**, with respect to all bond angles and lengths.

The Ru−Cl bond lengths for complexes which contain the $RuCl_2Ru$ fragment are usually close to 2.46 Å, and the Ru−Cl−Ru and Cl−Ru−Cl bond angles lie within the ranges 95.1–98.4 and 81.6–84.9 Å, respectively.[36–40] $[Ru(\mu\text{-}Cl)(PyP)_2]_2[OSO_2CF_3]_2$ has a Ru−Cl bond length of 2.48(14) Å, and Ru−Cl−Ru and Cl−Ru−Cl bond angles which fall just outside these values, 99.68(3) and 80.32(3)°, respectively. It is thought longer Ru···Ru distances are needed to allow dissociation of the dimer into the five-coordinate species, as has been observed for a similar compound with average Ru−Cl−Ru and Cl−Ru−Cl bond angles of 101.85 and 78.15°, respectively.[30]

Experiments with CO. The reactivity of both **2** and the ruthenium dimer **9** (containing the BPh_4^- counterion) with carbon monoxide was tested by monitoring a DCM-d_2 solution of each metal complex under an atmosphere of CO_g by NMR spectroscopy (in the case of **2** at −60 °C and room temperature and in the case of **9** at room temperature). The ^{1}H, ^{13}C, and ^{13}P NMR spectra indicated that at room temperature both **2** and **9** did indeed react cleanly with CO_g to form new products.

CO is a strongly binding ligand; hence it easily causes the dimeric **9** to dissociate into monomeric units by binding to the Ru center, most likely trans to the P donor atoms, forming complex **11** (Scheme 4). This was confirmed by the ^{31}P NMR spectrum, which shows a pair of doublets at 28.8 and 0.1 ppm (Hz coupling = 25.7). This splitting pattern is typical for inequivalent P atoms which are cis to each other. The chemical shifts exhibited here are comparable

(31) Khan, M. M. T.; Reddy, A. D. *Polyhedron* **1987**, *6*, 2009–2018.
(32) Bressan, M.; Rigo, P. *J. Inorg. Nucl. Chem.* **1976**, *38*, 592–593.
(33) Shen, J.-Y.; Slugovc, C.; Wiede, P.; Mereiter, K.; Schmid, R.; Kirchner, K. *Inorg. Chim. Acta* **1998**, *268*, 69–76.
(34) Appleton, T. G.; Clark, H. C.; Manzer, L. E. *Coord. Chem. Rev.* **1973**, *10*, 335–422.
(35) Coe, B. J.; Glenwright, S. J. *Coord. Chem. Rev.* **2000**, *203*, 5–80.
(36) Southern, T. G.; Dixneuf, P. H.; Marouille, Y. L.; Grandjean, D. *Inorg. Chem.* **1979**, *18*, 2987–2991.
(37) Teulon, P.; Roziere, J. *J. Organomet. Chem.* **1981**, *214*, 391–397.
(38) Deschamps, B.; Mathey, F.; Fischer, J.; Nelson, J. H. *Inorg. Chem.* **1984**, *23*, 3455–3462.

Scheme 4. All Experiments Performed at RT in CD_2Cl_2 unless Otherwise Stated

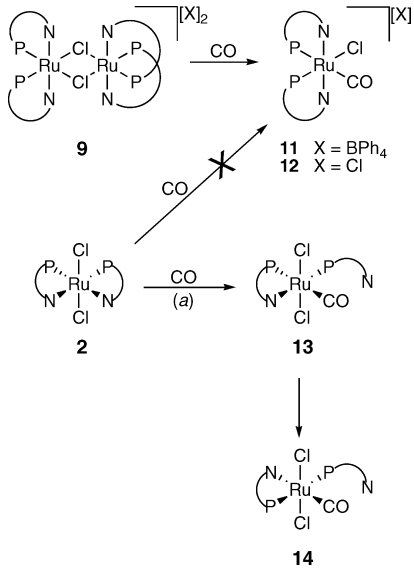

[a] Performed at RT and −60 °C.

to compounds similar to **11** which have been previously reported.[30] We saw no isomerization of **11**, even after 48 h at room temperature.

The initial ^{31}P NMR spectra of the reaction between CO and **2** exhibited a pair of doublets at 30.1 ppm and 1.8 ppm (Hz coupling = 30.2 Hz) which is indicative of inequivalent cis P atoms about the metal center, and similar to product **11** (or the analogous **12**). The ^{1}H NMR spectrum, however, was significantly different to that of **11**, which suggests the product is not **12** but **13**. Complex **13**, undergoes isomerization after only a few hours at room temperature, into the new product **14** (Scheme 4). This new isomer exhibited a pronounced AB splitting pattern in the $^{31}P\{^{1}H\}$ spectrum, with a pair of coupled doublets at 24.5 and 15.5 ppm (J_{PP} = 335.7 Hz). The $^{13}C\{^{1}H\}$ resonances of the carbonyl group of **14** appeared as a triplet in the ^{13}C NMR spectrum, with a chemical shift of 205.3 ppm (J_{CP} = 15.3 Hz). The splitting patterns exhibited in both the $^{31}P\{^{1}H\}$ and $^{13}C\{^{1}H\}$ spectra are indicative of a complex containing two inequivalent P atoms which are *trans* to each other and can best be attributed to a complex such as **14**.

Complex **14** was isolated when the reaction was performed on a large scale; the ruthenium complex **2** was stirred under an atmosphere of CO_g for 8 h, the subsequent removal of solvent yielded **14** as a yellow solid, as confirmed by electrospray mass spectroscopy. The mass spectrum exhibited a *m/z* peak for the positively charged ion $[RuCl_2(CO)(PyP)_2 + H]^+$; for such a species to exist the complex must contain one ligand bound through only one donor atom. The splitting pattern of the ^{31}P and ^{13}C NMR spectra indicate then that where one of the PyP ligands is pendant the P-donor atom remains bound to the metal center.

Conclusions

trans,*cis*,*cis*-$RuCl_2(PyP)_2$ (**2**), *cis*,*cis*,*cis*-$RuCl_2(PyP)_2$ (**3**), *cis*,*cis*,*cis*,*trans*-$RuCl_2(PyP)_2$ (**4**), *trans*,*cis*,*cis*-$OsCl_2(PyP)_2$ (**5**), and *cis*,*cis*,*trans*-$OsCl_2(PyP)_2$ (**6**) have been synthesized from PyP and $MCl_2(PPh_3)_3$ (where M = Ru or Os). This is the first example of three of the possible five stereoisomers of a complex of general formula $RuCl_2(P^{\frown}N)_2$ being synthesized. All five complexes were characterized by NMR spectroscopy and exhibited a certain amount of rigidity and steric hindrance about the ligands of the complexes in the solution state. Four of the complexes, **2**, **3**, **4**, and **5**, were also characterized by X-ray crystallography, which confirmed their geometry and showed negligible distortion from other similar literature compounds.

The isomerization of the Ru and Os complexes of the type $MCl_2(PyP)_2$ was investigated under a range of reaction conditions. The isomers formed in chlorinated solvents differed from those formed in ethanol. Tetrahydrofuran and acetone induced no isomerization in the complexes. The osmium analogue **5** of the ruthenium complex **2** exhibited similar isomerization processes which is unsurprising considering the similar spectroscopic and structural properties of **2** and **5**. Osmium complex **6**, however, was far more stable toward isomerization than the analogous ruthenium complex **4**; this could be due to the larger atomic radius of Os compared to Ru, which would decrease the degree of steric strain about the metal center. The bimetallic analogues of the above complexes, $[M(\mu\text{-}Cl(PyP)_2]_2[X]_2$ (where M = Ru or Os and X = OSO_2CF_3, BF_4 or BPh_4), (**7**–**10**), were synthesized either by addition of a silver salt at room temperature in dichloromethane or by addition of a sodium salt in EtOH at reflux to complexes **2** or **5**. No dissociation of the chloride of the starting material **2** or **5** was seen without the presence of counterion. The solid-state structures of these complexes were also determined using X-ray crystallography.

The isomerization of Ru isomers **2**, **3**, and **4** in solution could be due either to the hemilability of the bidentate PyP ligand or to dissociation and reassociation of the Cl^- ligand. If the PyP is hemilabile, the "opening" and subsequent recoordination of one ligand arm to a different position on the metal center could induce isomerization of the complex. It is generally observed that the N-donor is more weakly coordinating and, hence, is the most likely donor to labilize/recoordinate.[9,11] Dissociation and reassociation of the chloride anion would lead to the same product. In situ NMR studies of the reaction of **2** and **9** with carbon monoxide showed that these compounds react cleanly with CO. Complex **14**, which was formed from reaction with CO and **2**, exhibited dissociation of the N-donor atom of PyP and no dissociation of Cl^-. The reactivity of **2** with CO, and stability of the subsequent complex **14**, indicated that the mechanism of isomerization between the three isomers could be due to the hemilability of the PyP ligand. However, it is possible that hemilability of the PyP ligand might be induced only through binding of a strong donor ligand, such as carbon monoxide. Suppression of isomerization between the ruthenium complexes in the presence of excess chloride ions was observed through studies of solutions of **2** and **4** with tetrabutylammonium chloride. This indicates that the isomerization process most likely involves dissociation and rebinding of the Cl^- coligand, with the possibility of Ru−N bond dissociation also occurring.

(39) Kojima, T.; Matsuo, H.; Matsuda, Y. *Inorg. Chim. Acta* **2000**, *300–302*, 661–667.
(40) Marchenko, A. V.; Huffman, J. C.; Valerga, P.; Tenorio, M. J.; Puerta, M. C.; Caulton, K. G. *Inorg. Chem.* **2001**, *40*, 6444–6450.

Experimental Section

All reactions were performed under $N_{2(g)}$ or $Ar_{(g)}$. Solvents were purified and dried under $Ar_{(g)}$ using conventional methods.[41] Except where specified, chemicals were purchased from either Aldrich Chemical Co., Inc., Precious Metals Online PMO P/L, or Cambridge Isotope Laboratory and used as received unless otherwise stated. [*n*-Bu_4N]Cl·H_2O was recrystallized from acetone/Et_2O and dried in vacuo for 6 h. The ^1H, ^{31}P, and ^{13}C spectra were recorded on Bruker DPX300, DMX500, or DMX600 spectrometers. ^1H NMR and ^{13}C NMR chemical shifts were referenced internally to residual solvent resonances. ^{31}P NMR was referenced externally using H_3PO_4 (85% in D_2O) in a capillary taken to be at 0.0 ppm. ^{19}F was referenced externally using α,α,α-trifluorotoluene in $CDCl_3$. IR spectra were recorded using an ATI Mattson Genesis Series FTIR spectrometer or an Avatar 370 FTIR spectrometer as KBr disks. Elemental analyses were carried out at the Campbell Microanalytical Laboratory, University of Otago, New Zealand. Single-crystal X-ray analysis was performed by Dr. Matthew Smith and Dr. Anthony Willis at the Research School of Chemistry, Australian National University, Canberra. X-ray diffraction data were measured at 200 K on a Nonius KappaCCD diffractometer using Mo Kα radiation. Intensity data were collected with ψ and ω scans and corrected for absorption analytically. The structures were solved with the use of SIR92 and refined using the SHELXL-97 or CRYSTALS software packages. Mass spectra were acquired at the BioAnalytical Mass Spectrometry Facility (BMSF), University of New South Wales. ESI-MS were performed by Dr. Russel Pickford or Tharusha Jayasena using a Finnigan or Micromass QToF mass spectrometer. In reporting mass spectral data, M is defined as the molecular weight of the compound of interest. In the case of the ESI-MS of cationic compounds, M is defined as the molecular weight of the cationic fragments.

The ligand PyP[28] (**1**) and complexes $RuCl_2(PPh_3)_3$[42] and $OsCl_2(PPh_3)_3$[43] were synthesized by following the reported methods.

Synthesis of *trans*,*cis*,*cis*-$RuCl_2(PyP)_2$ (2). Dichloromethane (DCM) (50 mL) was added to a mixture of $RuCl_2(PPh_3)_3$ (1.060 g, 1.106 mmol) and PyP (0.628 g, 2.241 mmol) to produce a red solution which was stirred for 5 h. The solution was concentrated in vacuo and *n*-hexanes added to produce a yellow precipitate. The solid was collected by filtration, washed thoroughly with *n*-hexanes (3 × 10 mL), and dried in vacuo to give a yellow solid. Yield: 0.728 g, 90%.

The product was recrystallized from DCM/*n*-hexanes and then redissolved in DCM and filtered through celite. *n*-Hexanes was layered over the filtrate to give yellow plates suitable for X-ray crystallography.

Anal. Calcd for $C_{34}H_{34}Cl_2N_4P_2Ru·2H_2O$: C, 53.13; H, 4.98; N, 7.29. Found: C, 52.82; H, 4.69; N, 7.17. ^1H NMR (600 MHz, THF-d_8) δ 7.72 (d, $^3J_{(H4-H3)} = 1.8$ Hz, 2H, **H**5), 7.50 (m, 2H, **H**3), 7.33 (m, 8H, *o*-C **H** of PPh_2), 7.11 (apparent t, $J = 7.0$ Hz, 4H, *p*-C **H** of PPh_2), 6.95 (apparent t, $J = 7.5$ Hz, 4H, *m*-C **H** of PPh_2), 6.19 (apparent t, $^3J_{(H3-H4,H5-H4)} = 2.2$ Hz, 2H, **H**4), 5.39 (br s, 4H, NC $\mathbf{H}_2$), 2.65 (m, 4H, PC $\mathbf{H}_2$) ppm. $^{31}P\{^1H\}$ NMR (121 MHz, $CDCl_3$) δ 34.4 (s) ppm. $^{13}C\{^1H\}$ NMR (151 MHz, THF-d_8) δ 146.7 (s, **C**5), 139.8 (br s, *ipso*-**C** of PPh_2), 134.7 (apparent t, $J = 0.03$ Hz, *o*-C of PPh_2), 132.8 (s, **C**3), 128.4 (s, *p*-**C** of PPh_2), 126.8 (apparent t, $J = 0.03$ Hz, *m*-**C** of PPh_2), 104.4 (s, **C**4), 48.3 (s, N $\mathbf{C}H_2$), 34.6 (m, P $\mathbf{C}H_2$) ppm. ESI-MS (DCM), *m*/*z* (%): 732.1 (100) $[M^+]$. IR (KBr disk) υ 3022 (m), 1434 (s), 1098 (s), 744 (s), 696 (s), 522 (s) cm^{-1}.

Synthesis of *cis*,*cis*,*cis*-$RuCl_2(PyP)_2$ (3). PyP (0.254 g, 0.906 mmol) and $RuCl_2(PPh_3)_3$ (0.433 g, 0.452 mmol) were refluxed in toluene (30 mL) for 4 h, during which time the red suspension became tan colored. The mixture was filtered and the tan solid washed with EtOH (3 × 10 mL) and MeOH (2 × 10 mL). The combined washings were concentrated in vacuo, and Et_2O was sadded to precipitate out a yellow solid which was collected by filtration. The solid was recrystallized from DCM/Et_2O. Yield: 0.111 g, 34%.

Crystals suitable for X-ray crystallography were grown from DCM/*n*-pentane layering to give yellow cubes. (This method produced a mixture of crystals of both *trans*,*cis*,*cis*-$RuCl_2(PyP)_2$ and *cis*,*cis*,*cis*-$RuCl_2(PyP)_2$.)

Anal. Calcd for $C_{34}H_{34}Cl_2N_4P_2Ru·CH_2Cl_2$: C, 51.42; H, 4.44; N, 6.85. Found: C, 51.67; H, 4.88; N, 6.85. ^1H NMR (300 MHz $CDCl_3$) δ 9.07 (br d, $J = 1.9$ Hz, 1H, **H′**5), 8.30 (m, 2H, −C**H** of PPh_2), 7.72 (t, $J = 9.4$ Hz, 2H, −C**H** of PPh_2), 7.56 (br s, 1H, **H′**3), 7.40 (t, $J = 8.7$ Hz, 2H, −C**H** of PPh_2), 7.23–7.16 (m, 6H, **H**3 and −C**H** of PPh_2), 7.03–6.90 (m, 5H, −C**H** of PPh_2), 6.73 (m, 2H, −C**H** of PPh_2), 6.53 (d, $J = 1.9$ Hz, 1H, **H**5), 6.44–6.34 (m, 3H, **H′**4 and −C**H** of PPh_2), 5.86 (t, $J = 2.6$ Hz, 1H, **H**4), 5.53–5.40 (m, 1H, −NC′**H**), 5.22–5.08 (m, 1H, −NC**H**), 4.61–4.45 (m, 1H, −NC′**H**), 3.78–3.62 (m, 1H, −NC**H**), 3.12–2.99 (m, 1H, −PC**H**), 2.71–2.62 (m, 1H, −PC′**H**), 2.54–2.30 (m, 2H, −NC**H** and −NC′**H**) ppm. $^{31}P\{^1H\}$ NMR (121 MHz, $CDCl_3$) δ 35.9 (d, $^2J_{(P-P)} = 36.1$ Hz), 29.1 (d, $^2J_{(P-P)} = 37.0$ Hz) ppm. $^{13}C\{^1H\}$ NMR (150 MHz, CD_2Cl_2) δ 146.0 (m, **C**5 and **C′**5), 138.9–135.8 (m, 4 × *ipso*-**C** of PPh_2), 134.9 (s, $-\mathbf{C}_6H_5$), 134.3 (s, $-\mathbf{C}_6H_5$ or **C**3), 133.6 (s, **C′**3), 132.9 (d, $J = 8.7$ Hz, $-\mathbf{C}_6H_5$), 132.0 (d, $J = 8.43$ Hz, $-\mathbf{C}_6H_5$), 129.5 (s, $-\mathbf{C}_6H_5$ or **C**3), 129.0 (s, $-\mathbf{C}_6H_5$ or **C**3), 129.0 (s, $-\mathbf{C}_6H_5$), 127.8 (m, 2 × $-\mathbf{C}_6H_5$), 127.7 (d, $J = 9.5$ Hz, $-\mathbf{C}_6H_5$), 127.2 (s, $-\mathbf{C}_6H_5$ or **C**3), 127.1 (s, $-\mathbf{C}_6H_5$ or **C**3), 106.1 (s, **C**4), 105.7 (s, **C**′4), 47.2 (s, -N $\mathbf{C}H_2$ and -N **C**′H_2), 31.5 (d, $J = 25.6$ Hz, -P **C**′H_2), 23.7 (d, $J = 28.4$ Hz, ′-P$\mathbf{C}H_2$) ppm. ESI-MS (DCM), *m*/*z* (%): 663.3 (100) $[M - 2Cl]^+$, 697.0 (50) $[M - Cl]^+$, 732.0 (20) $[M]^+$. IR (KBr disk) υ 3643 (br), 3446 (br), 3053 (br), 1622 (s), 1434 (s), 1101 (s), 850 (s), 745 (s), 697 (s) cm^{-1}.

Synthesis of *cis*,*cis*,*trans*-$RuCl_2(PyP)_2$ (4). 2 (0.098 g, 0.134 mmol) was refluxed in EtOH for 1.25 h. The reaction mixture was evacuated to dryness to give a yellow solid. Yield: 0.083 g, 84%.

Crystals suitable for X-ray crystallography were grown from DCM/*n*-pentane layering to give yellow plates.

Anal. Calcd for $C_{34}H_{34}Cl_2N_4P_2Ru·H_2O·CH_2Cl_2$: C, 50.31; H, 4.58; N, 6.71. Found: C, 50.35; H, 4.58; N, 6.69. ^1H NMR (300 MHz CD_2Cl_2) δ 7.83 (d, $^3J_{(H4-H5)} = 1.3$ Hz, 2H, **H**5), 7.62 (d, $^3J_{(H4-H3)} = 2.2$ Hz, 2H, **H**3), 7.44 (m, 4H, *o*-C**H** of PPh), 7.32–7.11 (m, 8H, *m*-C**H** and *p*-C**H** of PPh, *p*-C **H** of PPh′), 6.94 (apparent t, $J = 7.3$ Hz, 4H, *m*-C**H** of PPh′), 6.24 (apparent t, $J = 8.2$ Hz, 4H, *o*-C**H** of PPh′), 6.13 (t, $^3J_{(H3-H4,H5-H4)} = 7.9$ Hz, 2H, **H**4), 5.82–5.70 (m, 2H, −NC**H**H′), 4.78–4.62 (m, 2H, −NCH**H′**), 2.80–2.56 (m, 4H, P$\mathbf{C}H_2$) ppm. $^{31}P\{^1H\}$ NMR (121 MHz, CD_2Cl_2) δ 32.7 (s) ppm. $^{13}C\{^1H\}$ NMR (151 MHz, CD_2Cl_2) δ 148.7 (s, **C**5), 137.8 (m, *ipso*-**C** of PPh_2), 136.3 (m, *ipso*-**C** of PPh_2), 134.7 (s, **C**3), 134.1(s, *o*-**C** of PPh), 130.4 (s, *o*-**C** of PPh′), 129.3 (s, *p*-**C** of PPh′), 129.0 (*p*-**C** of PPh), 128.5 (s, *m*-**C** of PPh′), 127.3 (s, *m*-**C** of PPh), 105.6 (s, **C**4), 48.4 (s, N $\mathbf{C}H_2$), 25.5 (m, P $\mathbf{C}H_2$) ppm. ESI-MS (DCM), *m*/*z* (%): 720.9 (100) $[RuCl(PyP)_2 + Na]^+$, 685.2 (20) $[Ru(PyP)_2 + Na]^+$. IR (KBr disk) υ 2957 (br s), 1434 (s), 104 (s), 852 (s), 757 (s), 698 (s) 534 (s) cm^{-1}.

(41) Perrin, D. D.; Armarego, W. L. F. *Purification of Laboratory Chemicals*, 3rd ed.; Pergamon Press: Oxford, 1993.
(42) Stephenson, T. A.; Wilkinson, G. *J. Inorg. Nucl. Chem.* **1966**, *28*, 945–956.
(43) Elliott, G. P.; Mcauley, N. M.; Roper, W. R. *Inorg, Synth.* **1989**, *26*, 184–189.

Synthesis of *trans*,*cis*,*cis*-$OsCl_2(PyP)_2$ (5). DCM (50 mL) was added to a mixture of $OsCl_2(PPh_3)_3$ (0.786 g, 0.750 mmol) and PyP (0.424 g, 1.51 mmol) to produce a brown solution which was stirred for 5 h. The solution was concentrated in vacuo and *n*-hexanes added to produce an olive-green precipitate. The solid was collected by filtration, washed thoroughly with *n*-hexanes (3 × 10 mL), and dried in vacuo to give an olive-green solid. Yield: 0.566 g, 92%.

Crystals suitable for X-ray crystallography were grown by DCM/*n*-hexanes layering to give yellow prisms.

Anal. Calcd for $C_{34}H_{34}Cl_2N_4P_2Os \cdot CH_2Cl_2$: C, 46.36; H 4.00; N, 6.18. Found: C, 46.61; H, 3.83; N, 6.07. ^{1}H NMR (300 MHz $CDCl_3$) δ 7.52 (d, $^3J_{(H4-H3)}$ = 2.0 Hz, 2H, **H**5), 7.33 (d, $^3J_{(H4-H3)}$ = 2.0 Hz, 2H, **H**3), 7.17–7.12 (m, 12H, *o*-C**H** of PPh_2, *p*-C**H** of PPh_2), 7.01 (apparent t, J = 7.7 Hz, 8H, *m*-C **H** of PPh_2), 6.24 (apparent t, $^3J_{(H3-H4,\ H5-H4)}$ = 2.7 Hz, 2H, **H**4), 5.29 (br s, 4H, NC$\mathbf{H}_2$), 2.67 (br s, 4H, PC $\mathbf{H}_2$) ppm. ^{31}P{^{1}H} NMR (121 MHz, $CDCl_3$) δ −28.2 (s) ppm. ^{13}C{^{1}H} NMR (125 MHz, CD_2Cl_2) δ 145.8 (s, **C**5), 139.8 (br s, *ipso*-**C** of PPh_2), 133.7 (s, *o*-**C** of PPh_2), 132.7 (s, **C**3), 128.4 (s, *p*-**C** of PPh_2), 126.7 (s, *m*-**C** of PPh_2), 104.8 (s, **C**4), 48.5 (s, N **C**H_2), 33.3 (br s, P **C**H_2) ppm. ESI-MS (DCM), *m*/*z* (%): 822.2 (100) [M^+]. IR (KBr disk) υ 3050 (m), 1434 (s), 1095 (s), 744 (s), 697 (s), 524 (s) cm^{-1}.

Synthesis of *cis*,*cis*,*trans*-$OsCl_2(PyP)_2$ (6). *trans*,*cis*,*cis*-$OsCl_2(PyP)_2$ (52.6 mg, 0.064) was refluxed in EtOH for 2 h. The solution was cooled to RT and concentrated in vacuo. Et_2O was added to the concentrated solution and the subsequent precipitate collected by filtration and dried in vacuo to give an olive-green solid. Yield: 33.5 mg, 64%.

Anal. Calcd for $C_{34}H_{34}Cl_2N_4OsP_2 \cdot 2H_2O$: C, 46.61; H, 4.47; N, 6.53. Found: C, 47.11; H, 4.45; N, 6.27. ^{1}H NMR (600 MHz CD_2Cl_2) δ 7.90 (s, 2H, **H**5) 7.54 (s, 2H, **H**3), 7.30 (m, 4H, *o*-C**H** of PPh), 7.23 (m, 2H, *p*-C**H** of PPh), 7.17 (m, 4H, *m*-C**H** of PPh), 7.09 (apparent t, J = 7.7 Hz, *p*-C**H** of PPh′), 6.92 (apparent t, J = 7.2 Hz, 4 **H**, *m*-CH of PPh′), 6.33 (apparent t, J = 7.7 Hz, 4H, *o*-C**H** of PPh′), 6.12 (s, 2H, **H**4), 5.59–5.53 (m, 2H, −NC**H**H′), 4.63–4.55 (m, 2H, −NCH**H**′), 2.94–2.88 (m, 2H, PC**H**H′), 2.55–2.50 (m, 2H, PCH **H**′) ppm. ^{31}P{^{1}H} NMR (121 MHz, CD_2Cl_2) δ −22.4 (s) ppm. ^{13}C{^{1}H} NMR (125 MHz, CD_2Cl_2) δ 147.6 (s, **C**5), 136.8 (m, *ipso*-**C** of PPh and PPh′), 133.2 (s, *o*-**C**H of PPh, **C**3), 130.1 (s, *o*-**C**H of PPh′), 128.5 (s, *p*-**C**H of PPh′), 128.2 (s, *p*-**C**H of PPh), 127.8 (s, *m*-**C**H of PPh′), 126.7 (s, *m*-**C**H of PPh), 105.0 (s, **C**4), 48.7 (s, −N**C**H_2), 26.2 (m, −P**C**H_2) ppm. ESI-MS (DCM), *m*/*z* (%): 810.9 (100) [$OsCl(PyP)_2$+Na]$^+$. IR (KBr disk) υ 3419 (m), 1434 (s), 1279 (s), 1127 (s), 1106 (s), 697 (s), 746 (s), 698 (s) cm^{-1}.

Methods for Synthesis of [Ru(μ-Cl)$(PyP)_2]_2[X]_2$. (1a) Synthesis of [Ru(μ-Cl)$(PyP)_2]_2[OSO_2CF_3]_2$ (7) Using $AgOSO_2CF_3$. Silver triflate (76.6 mg, 0.299 mmol) was added to a solution of **2** (0.219 g, 0.299 mmol) in DCM. The solution was stirred for 3 h, during which time it became cloudy. The reaction mixture was filtered through celite and the filtrate concentrated in vacuo. *n*-Hexanes was added to produce a dark yellow precipitate which was collected by filtration, washed with *n*-hexanes (3 × 3 mL), and dried in vacuo. Yield: 0.184 g, 72%.

Crystals suitable for X-ray crystallography were grown by DCM/*n*-hexanes layering to give yellow prisms.

Anal. Calcd for $C_{70}H_{68}Cl_2F_6N_8O_6P_4Ru_2S_2$: C, 49.68; H, 4.05; N, 6.62. Found: C, 49.54; H, 4.09; N, 6.45. ^{1}H NMR (300 MHz, CD_2Cl_2) δ 7.74 (d, $^3J_{(H4-H3)}$ = 2.2 Hz, 4H, **H**3), 7.48 (t, J = 7.5 Hz, 4H, *p*-C**H** of PPh′), 7.36 (apparent t, J = 7.5 Hz, 8H, *m*-C **H** of PPh′), 7.21 (m, 8H, *o*-C**H** of PPh′), 7.13 (t, J = 7.3 Hz, 4H, *p*-C**H** of PPh), 6.92 (apparent t, J = 7.5 Hz, 8H, *m*-C**H** of PPh), 6.67 (d, $^3J_{(H4-H5)}$ = 2.0 Hz, 4H, **H**5), 5.85 (br s, 8H, *o*-C**H** of PPh′), 5.77 (t, $^3J_{(H5-H4,\ H3-H4)}$ = 2.7 Hz, 4H, **H**4), 5.10–4.93 (m, 8H, NC$\mathbf{H}_2$), 2.59 (m, 8H, PC$\mathbf{H}_2$) ppm. ^{31}P{^{1}H} NMR (121 MHz, CD_2Cl_2) δ 35.1 (s) ppm. ^{13}C{^{1}H} NMR (125 MHz, CD_2Cl_2) δ 146.5 (s, **C**3/5), 135.4 (s, **C**3/5), 134.5 (m, *ipso*-**C** of PPh′), 133.2 (s, *m*- or *p*-**C**H of PPh′), 131.3 (m, *ipso*-**C** of PPh′), 130.1 (s, *o*-**C**H of PPh′), 130.0 (s, *o*-**C**H of PPh′), 129.6 (m, *m*- or *p*-**C**H of PPh′), 128.6 (s, *m*- or *p*-**C**H of PPh′), 127.5 (s, *m*- or p-**C**H of PPh′), 106.6 (s, **C**4), 47.7 (s, N**C**H_2), 24.9 (m, P**C**H_2) ppm. ^{19}F NMR (282 MHz, CD_2Cl_2) δ −79.10 ppm. ESI-MS (DCM), *m*/*z* (%): 1325.9 (60) [M − 2Cl + H]$^+$, 748.09 (100). MALDI-TOF, *m*/*z* (%): 697.2 (65) [$RuCl(PyP)_2]^+$, 811.2 (95), 850.3 (100). IR (KBr disk) υ 2958 (m), 2926 (m), 1634 (w), 1435 (s), 1279 (m), 1260 (m), 1031 (s), 698 (s), 638 (s) cm^{-1}.

(1b) Synthesis of [Ru(μ-Cl)$PyP)_2]_2[BF_4]_2$ (8) Using $AgBF_4$. Method is the same as in (1a), but $AgBF_4$ was used in place of $AgOSO_2CF_3$. Yield: 83%.

Anal. Calcd for $C_{80}H_{78}B_2Cl_2F_8N_8P_4Ru_2$: C, 52.09; H, 4.37; N, 7.15. Found: C, 51.78; H, 4.51; N, 7.16. ^{31}P{^{1}H} NMR (121 MHz, CD_2Cl_2) δ 35.0 (s) ppm. ^{19}F NMR (282 MHz, CD_2Cl_2) δ −153.11 ppm. ESI-MS (DCM), *m*/*z* (%): 748.03 (100). IR (KBr disk) υ 2963 (m), 1634 (w), 1434 (s), 1262 (s), 1084 (s), 852 (s), 804 (s), 747 (s), 698 (s) cm^{-1}.

(2a) Synthesis of [Ru(μ-Cl)$(PyP)_2]_2[BPh_4]_2$ (9) using $NaBPh_4$ in EtOH. 2 (0.159 g, 0.217 mmol) and $NaBPh_4$ (0.821 g, 0.240 mmol) were refluxed in EtOH for 3.5 h. The resulting suspension was cooled to RT and the solvent removed in vacuo. The residue was suspended in DCM and filtered through celite. The filtrate was concentrated in vacuo and *n*-hexanes added to precipitate out a yellow solid which was washed with *n*-hexanes (2 × 2 mL) and dried in vacuo. Yield: 0.179 g, 81%.

Anal. Calcd for $C_{116}H_{108}B_2Cl_2N_8P_4Ru_2$: C, 68.54; H, 5.36; N, 5.51. Found: C, 68.25; H, 5.50; N, 5.54. ^{31}P{^{1}H} NMR (121 MHz, CD_2Cl_2) δ 34.8 (s) ppm. ESI-MS (DCM), *m*/*z* (%): 748.03 (100), 721 (40), 697 (40) [M − Cl]$^+$. MALDI-TOF (DCM), *m*/*z* (%): 697.11 (75) [$Ru(PyP)_2Cl]^+$, 850.18 (100). IR (KBr disk) υ 3053 (br s), 1479 (s), 1434 (s), 1105 (s), 854 (s), 745 (s), 703 (s) cm^{-1}.

Synthesis of [Os(μ-Cl)$(PyP)_2]_2[BPh_4]_2$ (10). $NaBPh_4$ (89 mg, 0.260 mmol) was added to a suspension of *trans*,*cis*,*cis*-$OsCl_2(PyP)_2$ (0.193 g, 0.235 mmol) in EtOH (30 mL). The mixture was refluxed for 3 h and then cooled to RT. The solid was collected by filtration and washed with acetone (7 × 10 mL) to leave behind a white solid. The washings were combined and evacuated to dryness in vacuo to give a yellow/green solid. Yield: 0.173 g, 67%.

Crystals suitable for X-ray crystallography were grown from acetone/*n*-pentane layering to give orange plates.

Anal. Calcd for $C_{116}H_{108}B_2Cl_2N_8Os_2P_4$: C, 63.01; H, 4.92; N, 5.07. Found: C, 62.41; H, 5.04; N, 5.09. ^{1}H NMR (500 MHz, $(CD_3)_2CO$) δ 7.78 (d, ^3J = 2.3 Hz, 4H, **H**3), 7.53–7.46 (m, 12H, *p*-C**H** and *m*-C**H** of PPh), 7.36–7.33 (m, 16H, *o*-C**H** of BPh_4), 7.27 (apparent t, J = 8.5 Hz, 8H, *o*-C**H** of PPh), 7.18 (apparent t, J = 7.5 Hz, 4H, *p*-C**H** of PPh′), 6.99 (m, 8H, *m*-C**H** of PPh′), 6.92 (apparent t, J = 7.4 Hz, 16H, *m*-C**H** of BPh_4), 6.83 (d, ^3J = 2.1 Hz, 4H, **H**5), 6.78 (t, J = 7.2 Hz, 8H, *p*-C**H** of BPh_4), 6.08 (m, 8H, *o*-C**H** of PPh′), 5.84 (t, $^3J_{(H3-H4,H5-H4)}$ = 2.6 Hz, 4H, **H**4), 5.15–4.99 (m, 8H, NC$\mathbf{H}_2$), 2.90–2.84 (m, 4H, PC**H**H′), 2.72–2.66 (m, 4H, PCH **H**′) ppm. ^{31}P{^{1}H} NMR (202 MHz, CD_2Cl_2) δ −20.5 (s) ppm. ^{13}C{^{1}H} NMR (125 MHz, $(CD_3)_2CO$) δ 163.9 (q, $^1J_{(B-C)}$ = 49.60, *ipso*-**C** of BPh_4), 145.8 (s, **C**5), 136.1 (s, *o*-**C** of BPh_4), 135.0 (s, **C**3), 134.5 (s, *ipso*-**C** of PPh), 132.9 (s, *o*-**C**H of PPh), 132.3 (s, *ipso*-**C** of PPh′), 129.7 (s, *m*-**C**H of PPh), 129.7 (s, *p*-**C**H of PPh′), 128.4 (s, *m*-**C**H of PPh′), 127.5 (s, *p*-**C**H of PPh), 125.0 (s, *m*-**C**H of BPh_4), 121.3 (s, *p*-**C**H of BPh_4), 106.2 (s, **C**4), 48.3

(s, N **C**H_2), 25.4 (m, P **C**H_2) ppm. MALDI-TOF, *m*/*z* (%): 787.3 (80) $[OsCl(PyP)_2]^+$, 940.4 (100). IR (KBr disk) υ 3052 (br s), 1481 (s), 1434 (s), 1262 (s), 1012 (s), 1031 (s), 852 (s), 745 (s), 700 (s) cm^{-1}.

Synthesis of $RuCl_2(CO)(\kappa^1$-*P*-PyP)(κ^2-*P*,*N*-PyP) (14). *trans*,*cis*,*cis*-$RuCl_2(PyP)_2$ (0.145 g, 0.198 mmol) was dissolved in DCM and the solution degassed via one cycle of freeze−vacuum−thaw. The atmosphere of the flask was replaced with $CO_{(g)}$ from a balloon, and the solution was stirred for 8 h under this atmosphere. The solution was evacuated to dryness to give a yellow solid. Yield: 0.094 g, 62%.

^{1}H NMR (600 MHz, CD_2Cl_2) δ 7.78–7.75 (m, 4H, Ar **H**), 7.70–7.66 (m, 4H, Ar **H**), 7.44–7.34 (m, 15H, 12 × Ar**H** and 3 × Py**H**), 7.21 (d, J = 2.1 Hz, Py**H**), 6.16 (apparent t, J = 1.92 Hz, 1H, **H**4), 5.88 (apparent t, J = 2.4 Hz, **H**4), 5.17–5.12 (m, 2H, NC′$\mathbf{H}_2$), 4.31–4.27 (m, 2H, NC$\mathbf{H}_2$), 3.24–3.20 (m, 2H, PC$\mathbf{H}_2$), 2.28–2.73 (m, 2H, PC′$\mathbf{H}_2$) ppm. ^{31}P{^{1}H} NMR (242 MHz, CD_2Cl_2) δ 24.5, 15.5 (AB spin system, J = 335.7 Hz) ppm. ^{13}C{^{1}H} NMR (150 MHz, CD_2Cl_2) δ 205.3 (apparent t, J = 15.3 Hz, **C**O), 147.3 (s, Py**C**), 139.4 (s, Py**C**), 134.3 (d, J = 8.9 Hz, Ar**C**), 133.7 (m, 1 × Ar**C** and 1 × Py**C**) 133.3 (m, *ipso*-**C** of PPh_2), 132.9 (m, *ipso*-**C** of PPh_2), 130.5 (s, Py**C**), 131.7 (s, Py**C**) 128.6 (d, J = 9.3 Hz, Ar**C**), 128.4 (d, J = 9.7, Ar**C**), 105.7 (s, **C**4), 105.5 (s, **C**4), 47.9 (s, N**C**H_2), 47.7 (s, N**C**′H_2), 28.7 (d, J = 21.7 Hz, P**C**′H_2), 28.3 (d, J = 23.7 Hz, P**C**H_2) ppm. ESI-MS (DCM), *m*/*z* (%): 725.0 (100) $[RuCl(CO)(PyP)_2]^+$, 761.0 (50) $[RuCl_2(CO)(PyP)_2 + H]^+$. IR (KBr disk) υ 1950 (CO) cm^{-1}.

Experiments with [*n*-Bu_4N]Cl. A CD_2Cl_2 solution of *cis*,*cis*,*trans*-$RuCl_2(PyP)_2$ and a CD_2Cl_2 solution of *cis*,*cis*,*trans*-$RuCl_2(PyP)_2$ and [*n*-Bu_4N]Cl (exs) combined were monitored by ^{1}H NMR and ^{31}P{^{1}H} NMR spectroscopy; spectra were aquired every 24 h for 7 days.

A suspension of *trans*,*cis*,*cis*-$RuCl_2(PyP)_2$ (26.4 mg, 0.036 mmol) in EtOH (10 mL) and a suspension of *trans*,*cis*,*cis*-$RuCl_2(PyP)_2$ (26.6 mg, 0.036 mmol) and [*n*-Bu_4N]Cl (26.0 mg, 0.094 mmol) combined in EtOH (10 mL) were stirred for 5 h and then evacuated to dryness to give orange residues. ^{1}H NMR and ^{31}P{^{1}H} spectra of the residues in CD_2Cl_2 were aquired. The two residues were resuspended in EtOH (10 mL) and stirred for 22 h to give clear solutions which were evacuated to dryness to give orange residues. ^{1}H NMR and ^{31}P{^{1}H} spectra of the residues in CD_2Cl_2 were acquired.

Acknowledgment. Financial support from the Australian Research Council and The University of New South Wales is gratefully acknowledged. S.L.D. wishes to thank the Australian government for an Australian Postgraduate Award scholarship.

Supporting Information Available: Crystallographic data in CIF format for complexes **2**, **3**, **4**, **5**, **6**, and **9**. This material is available free of charge via the Internet at http://pubs.acs.org.

IC7019044